

---

This is an electronic reprint of the original article.  
This reprint may differ from the original in pagination and typographic detail.

Chang, Bo; Zhou, Quan; Ras, Robin H A; Shah, Ali; Wu, Zhigang; Hjort, Klas  
**Sliding droplets on hydrophilic/superhydrophobic patterned surfaces for liquid deposition**

*Published in:*  
Applied Physics Letters

*DOI:*  
[10.1063/1.4947008](https://doi.org/10.1063/1.4947008)

Published: 11/04/2016

*Document Version*  
Publisher's PDF, also known as Version of record

*Please cite the original version:*  
Chang, B., Zhou, Q., Ras, R. H. A., Shah, A., Wu, Z., & Hjort, K. (2016). Sliding droplets on hydrophilic/superhydrophobic patterned surfaces for liquid deposition. *Applied Physics Letters*, 108(15), 1-4. Article 154102. <https://doi.org/10.1063/1.4947008>

# Sliding droplets on hydrophilic/superhydrophobic patterned surfaces for liquid deposition

Bo Chang, Quan Zhou, Robin H. A. Ras, Ali Shah, Zhigang Wu, and Klas Hjort

Citation: *Appl. Phys. Lett.* **108**, 154102 (2016); doi: 10.1063/1.4947008

View online: <https://doi.org/10.1063/1.4947008>

View Table of Contents: <http://aip.scitation.org/toc/apl/108/15>

Published by the [American Institute of Physics](#)

---

## Articles you may be interested in

[Self-propelled droplet behavior during condensation on superhydrophobic surfaces](#)

*Applied Physics Letters* **108**, 194103 (2016); 10.1063/1.4949010

[Bulk water freezing dynamics on superhydrophobic surfaces](#)

*Applied Physics Letters* **110**, 041604 (2017); 10.1063/1.4974296

[Jumping-droplet electrostatic energy harvesting](#)

*Applied Physics Letters* **105**, 013111 (2014); 10.1063/1.4886798

[Facile stamp patterning method for superhydrophilic/superhydrophobic surfaces](#)

*Applied Physics Letters* **107**, 201606 (2015); 10.1063/1.4936177

[A model for contact angle hysteresis](#)

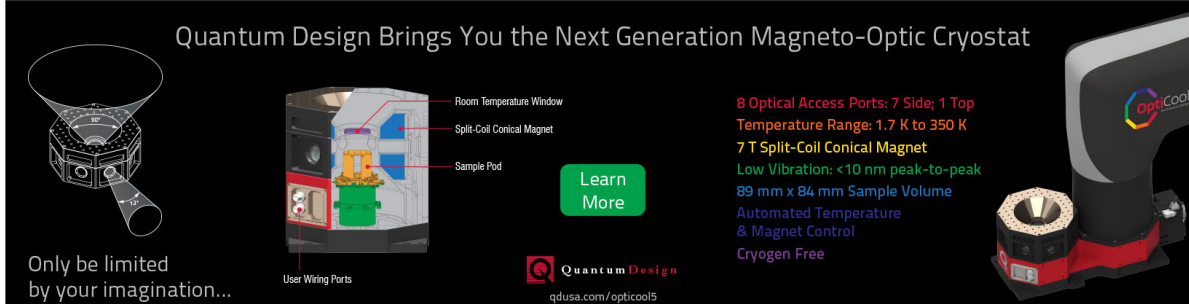
*The Journal of Chemical Physics* **81**, 552 (1984); 10.1063/1.447337

[Capillary-driven self-assembly of microchips on oleophilic/oleophobic patterned surface using adhesive droplet in ambient air](#)

*Applied Physics Letters* **99**, 034104 (2011); 10.1063/1.3615053

---

Quantum Design Brings You the Next Generation Magneto-Optic Cryostat



Only be limited by your imagination...

Room Temperature Window  
Split-Coil Conical Magnet  
Sample Pod  
User Wiring Ports

Learn More

Quantum Design  
qdusa.com/opticool5

8 Optical Access Ports: 7 Side; 1 Top  
Temperature Range: 1.7 K to 350 K  
7 T Split-Coil Conical Magnet  
Low Vibration: <10 nm peak-to-peak  
89 mm x 84 mm Sample Volume  
Automated Temperature & Magnet Control  
Cryogen Free

OptiCool

# Sliding droplets on hydrophilic/superhydrophobic patterned surfaces for liquid deposition

Bo Chang,<sup>1,2,a)</sup> Quan Zhou,<sup>3</sup> Robin H. A. Ras,<sup>1</sup> Ali Shah,<sup>4</sup> Zhigang Wu,<sup>2,5</sup> and Klas Hjort<sup>2</sup>

<sup>1</sup>Department of Applied Physics, School of Science, Aalto University, FI-02150 Espoo, Finland

<sup>2</sup>Department of Engineering Sciences, Uppsala University, SE-75121 Uppsala, Sweden

<sup>3</sup>Department of Electrical Engineering and Automation, School of Electrical Engineering, Aalto University, FI-00076 Espoo, Finland

<sup>4</sup>Department of Micro- and Nanosciences, Aalto University, FI-00076 Espoo, Finland

<sup>5</sup>State Key Laboratory of Digital Manufacturing Equipment and Technology, Huazhong University of Science and Technology, Wuhan 430074, China

(Received 22 January 2016; accepted 5 April 2016; published online 15 April 2016)

A facile gravity-induced sliding droplets method is reported for deposition of nanoliter sized droplets on hydrophilic/superhydrophobic patterned surface. The deposition process is parallel where multiple different liquids can be deposited simultaneously. The process is also high-throughput, having a great potential to be scaled up by increasing the size of the substrate. *Published by AIP Publishing.*  
[\[http://dx.doi.org/10.1063/1.4947008\]](http://dx.doi.org/10.1063/1.4947008)

Nanoliter sized droplet deposition is essential in many biomedical, chemical, and microfluidic applications, including droplet based microfluidic systems,<sup>1,2</sup> delivery of DNA,<sup>3</sup> DNA microarrays,<sup>4</sup> cell screening,<sup>5</sup> protein chips,<sup>6</sup> and material synthesis.<sup>7</sup> There are several techniques for droplet deposition, including contact<sup>8</sup> and non-contact dispensing technique,<sup>9</sup> dip-pen nanolithography,<sup>10–13</sup> and liquid deposition using patterned hydrophilic/hydrophobic surfaces<sup>14,15</sup> including dip-coating.<sup>16–19</sup> Dip-coating is a high-throughput method, depositing massive number of droplets in a short time,<sup>17</sup> though does not allow deposition of different liquids on individual deposition sites. On the other hand, all other methods allow deposition of different liquids on desired deposition sites. However, they are based on direct deposition of liquid on substrates,<sup>9,11</sup> which requires each deposition site being addressed by individual heads of the dispensing device, where the deposition throughput is linear to the speed of the device. By increasing the number of operating dispensing heads, the speed can be increased linearly at the expense of associated device complexity and fabrication costs.<sup>9</sup>

In this paper, we introduce a facile gravity-induced sliding droplets method for rapid and high-throughput deposition of droplets which can break this linear relation between the deposition throughput and the speed of dispensing device. The deposition throughput can be scaled linearly by the size of substrate without increasing the dispensing speed. We employ sliding droplets on an inclined patterned hydrophilic/superhydrophobic surface, where a nanoliter-range liquid volume is deposited on the hydrophilic pads. The motion of droplet has been extensively studied on superhydrophobic surfaces in general,<sup>20–25</sup> and a few studies also report on droplet motion on patterned hydrophilic/hydrophobic surfaces.<sup>15,26–30</sup> However, the motion of a droplet moving on patterned hydrophilic/superhydrophobic surfaces remains unexplored. We characterize the motion of a droplet sliding on a patterned hydrophilic/superhydrophobic surface by investigating the speed of the droplet and the deposited

volume on hydrophilic pads. We also demonstrate that the method can be used for parallel nanoliter deposition using different liquids. The proposed method is simple to apply and scalable, where the system only involves droplets and patterned hydrophilic/superhydrophobic surfaces.

A sketch of the proposed deposition method is presented in Fig. 1. A substrate containing a matrix of hydrophilic pads with superhydrophobic background is placed on a motorized rotational stage; different kinds of liquids are dispensed on the first row of the hydrophilic pads as shown in Fig. 1(a). The details of the deposition process are zoomed in Fig. 1(b). The substrate is then tilted and droplets start sliding by gravity. Each droplet follows the path of its corresponding column of hydrophilic pads, which are coated by the corresponding liquid due to large wetting contrast between hydrophilic pad and superhydrophobic background. During the sliding process, the rear edge of the droplet is repeatedly pinned and depinned (see Fig. 1(c)) from the hydrophilic pads. As the rear edge of the droplet transforms from the pinning state (zoomed view in Fig. 1(d)) to the depinned, part of the droplet is deposited on the hydrophilic pad.

When a droplet is moving on an inclined hydrophilic/superhydrophobic patterned surface, the major forces acting on the droplet include contact line pinning force, gravitational force, and viscous force. According to Macdougall and Ockrent,<sup>31</sup> the pinning force preventing the droplet sliding down is caused by contact angle hysteresis and unbalanced Young's force, which can be described as  $F_Y = L \cdot \gamma_{LV} \cdot (\cos \theta_r - \cos \theta_a)$ , where  $L$  is the width of the droplet and it is perpendicular to the droplet moving direction,  $\gamma_{LV}$  is the surface tension of the liquid, and  $\theta_a$  and  $\theta_r$  are the advancing and receding contact angle at the downhill and uphill edges of the contact line. In our analysis, viscous forces are negligible, because the droplet is mainly sliding on the surface and there is no obvious viscous flow observed within the droplet in our experiments, in agreement with the previous report.<sup>32</sup> The movement of a droplet on a hydrophilic/superhydrophobic surface was simulated using Matlab Simulink.

<sup>a)</sup> Author to whom correspondence should be addressed. Electronic mail: bo.chang@aalto.fi

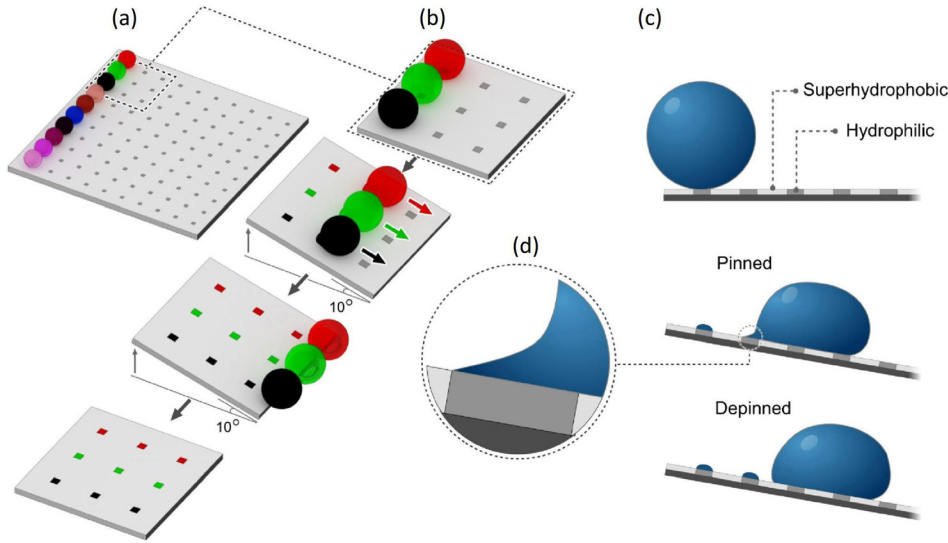


FIG. 1. Sketch and illustration of deposition by sliding droplets on patterned hydrophilic/superhydrophobic surface: (a) different kinds of liquids are placed on the first row of a  $10 \times 10$  matrix of hydrophilic pads surrounded by superhydrophobic substrate; (b) zoomed view of sliding droplets deposition process; (c) side view of a droplet sliding on a patterned surface; (d) zoomed view of the rear edge of the contact line pinned on the hydrophilic pad.

As shown in Figs. 2(a) and 2(b), when the rear edge of the contact line is pinned on the hydrophilic pad, the contact line starts to elongate and a small tail forms. At this state, the pinning force includes two parts: one part is the pinning force on superhydrophobic surface  $F_{Y1}$  and another is the pinning force on the pad  $F_{Y2}$ . The total pinning force is the sum of two

$$F_{Y1} + F_{Y2} = L\gamma_{LV}(\cos \theta_r - \cos \theta_a) + l\gamma_{LV}(\cos \theta_p - \cos \theta_r), \quad (1)$$

where  $F_{Y1} = (L - l)\gamma_{LV}(\cos \theta_r - \cos \theta_a)$ ,  $F_{Y2} = l\gamma_{LV}(\cos \theta_p - \cos \theta_r)$ ,  $L$  and  $l$  are the width of the droplet and

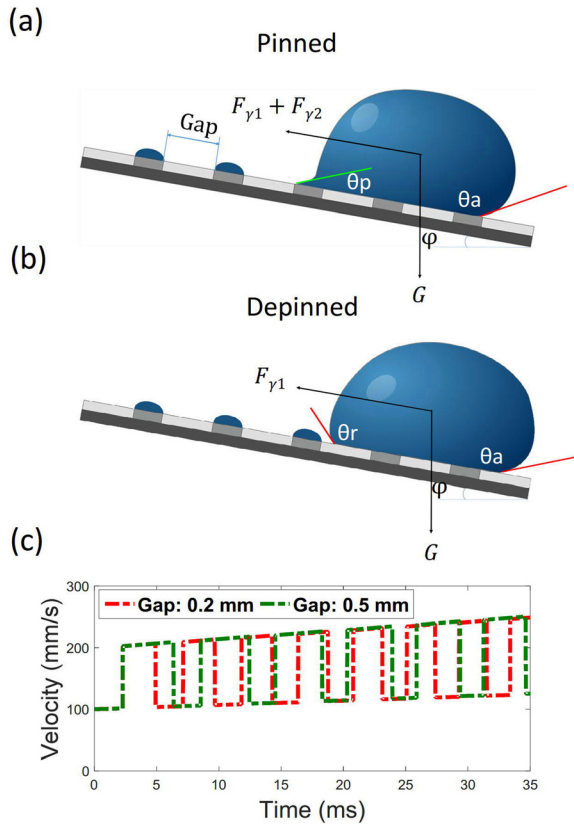


FIG. 2. Force configuration and simulation: (a) and (b) force configuration of a pinned and depinned droplet on a hydrophilic/superhydrophobic patterned surface; (c) calculated velocity as a function of time.

hydrophilic pad, respectively,  $\theta_p$  is the rear contact angle on the hydrophilic pad, varying between the advancing contact angle and the receding contact angle of the pad.

Based on the gravitational force and the varying pinning force, the total force acting on the droplet can be calculated, and the acceleration and velocity of the droplet can be derived. We simulated the motion of a 0.15 ml droplet sliding on a  $10^\circ$  tilted hydrophilic/superhydrophobic substrate, having a column of  $0.5 \text{ mm} \times 0.5 \text{ mm}$  pads with 0.2 mm and 0.5 mm gaps. The simulated velocity of the droplet is shown in Fig. 2(c). The results show that the droplet periodically speeds up and down according to the size of the hydrophilic pad and the distance between two pads. When the rear edge of the contact line is pinned on the hydrophilic pad, the velocity drops, and as the edge of the droplet is depinned from the pad, the velocity increases. The gap size has an obvious influence on the velocity, with a smaller gap size leading to more frequent fluctuations in velocity.

Experimental tests were carried out on a hydrophilic/superhydrophobic patterned surface, which consists of  $0.5 \text{ mm} (L) \times 0.5 \text{ mm} (W)$  hydrophilic black silicon pads and black silicon substrate coated with fluorocarbon polymer. The measured advancing contact angle on the substrate and the pad is  $170^\circ$  and  $30^\circ$ , respectively. The details of the fabrication process are reported in the supplementary material.<sup>33</sup> The sliding droplet deposition process was characterized with a high-speed video camera (Phantom Miro M-310), and images were analyzed by image processing algorithms in MATLAB, see Figs. 3(a) and 3(b). The velocity of the droplet was estimated based on the trajectory of the contact line center (Fig. 3(b)), and the amount of the deposition was estimated using the same images.

The sliding droplet deposition in Fig. 3 is on a substrate with gaps between hydrophilic pads of 0.2 mm. The rear edge of the droplet was pinned on one pad for about 4 ms (see multimedia view of Figs. 3(a) and 3(b)). The velocity of the sliding droplet was observed to fluctuate periodically, where an average of five sets of the experimental data is compared with the simulation in Fig. 3(c), following well the trend of the theoretical estimation. The average speed of droplet was also analyzed for tilt angle  $a$  of  $10^\circ$ ,  $20^\circ$ ,  $30^\circ$ ,  $40^\circ$ , and  $50^\circ$ . The

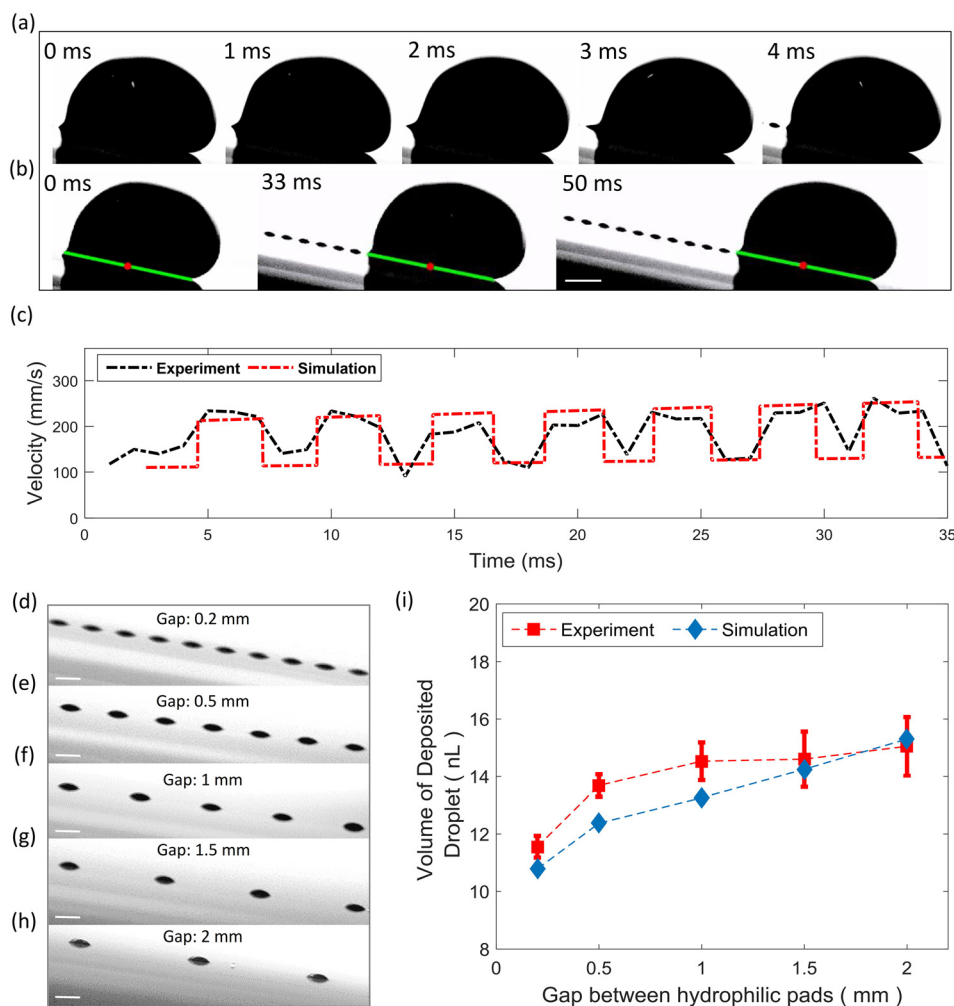


FIG. 3. Characterization of a droplet sliding on a patterned hydrophilic/superhydrophobic surface tilted at  $10^\circ$ : (a) and (b) side view images of a sliding droplet on patterned surface with detected contact line (green line) and center (red dot), scale bar 2 mm; (c) comparison of the simulated velocity with the average of experimental data; (d)–(h) deposited droplets on pads of  $0.5\text{ mm} \times 0.5\text{ mm}$  and with gap of 0.2 mm, 0.5 mm, 1 mm, 1.5 mm, and 2 mm, scale bars 0.5 mm; (i) volume of deposited droplet as a function of gap between pads. (Multimedia view) [URL: <http://dx.doi.org/10.1063/1.4947008.1>]

calculated capillary number  $Ca$  has linear relationship with  $\text{Bo} \sin(\alpha)$  as shown in Fig. S2 of supplementary material,<sup>33</sup> which is in consistent with an earlier report.<sup>30</sup>

We varied the gap from 0.2 mm to 2 mm to investigate its influence on the deposited volume. Figs. 3(d)–3(h) show the images of the deposited droplets on hydrophilic pads with different gaps. The relationship between the volume of deposited droplet and the size of the gap between the pads is presented in Fig. 3(i), where each test was repeated 6 times. The results show that 11–16 nL deposition with a standard deviation of 0.5–1.5 nL can be achieved on patterned hydrophilic/superhydrophobic surfaces. When the gap is 0.2 mm, the deposition is  $11.5 \pm 0.5$  nL. The deposited volume increases slightly with larger gap sizes, and the standard deviation increases to 1.5 nL.

The results agree reasonable well with the simulation using HyDro,<sup>34</sup> as indicated in Fig. 3(i). In the simulation, we noticed that the neck between the small and the large droplet is longer with larger gaps, and the breaking point of the neck is further away from the hydrophilic pad, leading to greater volume of the deposition on the pad.

The sliding droplet deposition was demonstrated by liquid patterning and parallel deposition. Samples with different shapes of hydrophilic pads have been fabricated, where the results are highlighted in Fig. 4. Figs. 4(a) and 4(b) show the detailed features in the logo of Uppsala

University and a flower-shaped pad visualized by the sliding droplet. The possibility of parallel deposition was also tested. Water droplets dyed in different colors were dispensed (see multimedia view of Fig. 4(c)) and deposited (Fig. 4(d)) on the sample. Additionally, the proposed deposition method is scalable. Taking the parameters used in the experiments (pad size:  $500\text{ }\mu\text{m}$ , gap size:  $200\text{ }\mu\text{m}$ , average speed of the sliding droplet:  $200\text{ mm/s}$ , size of the sliding droplet: 0.15 ml, deposited volume on each pad: 15 nL), a single sliding droplet can deposit 1000 pads in just 3.5 s. The throughput can be further scaled up using the parallel deposition method proposed in the paper, which leads to 10 000 deposition with 10 simultaneously sliding droplets in 3.5 s. This shows the great potential of the proposed method for large scale and high-density liquid deposition.

In summary, a simple deposition method was presented, utilizing moving droplets on patterned hydrophilic/superhydrophobic surface to achieve parallel deposition. The combination of a good wetting property of the pads and superhydrophobicity of the substrate, as well as reasonable gaps between the pads, can lead to deposition with uniformity better than 5%. The proposed method should also be applicable to other substrates such as glass or polymer, provided hydrophilic/superhydrophobic patterns can be produced on the substrate. Additionally, the method can be used for parallel deposition using multiple different liquids.



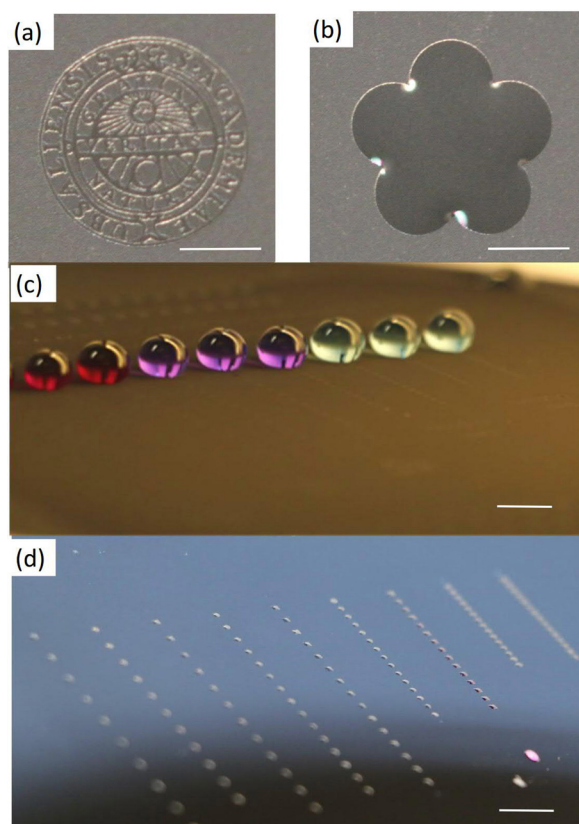


FIG. 4. Liquid patterning and parallel droplets deposition: (a) a logo of Uppsala University visualized with water, scale bar 1 mm; (b) a flower-shaped pad filled with water, scale bar 1 mm; (c) and (d) parallel deposition using different colored liquids on  $0.5 \times 0.5$  mm pads, scale bars 1 cm. (Multimedia view) [URL: <http://dx.doi.org/10.1063/1.4947008.2>]

This research was supported by the Academy of Finland's Centres of Excellence Programme (HYBER, 2014-2019), the Academy of Finland (Grant No. 275117), Aalto Energy Efficiency Programme (Project MOPPI, 2012-2016). The authors would like to thank Aalto Nanofabrication Center at Micronova (Espoo, Finland) for provision of facilities and Andreas Dahlin for drawing the sketch of the liquid deposition method.

<sup>1</sup>G. M. Whitesides, *Nature* **442**, 368 (2006).

<sup>2</sup>J. J. Agresti, E. Antipov, A. R. Abate, K. Ahn, A. C. Rowat, J.-C. Baret, M. Marquez, A. M. Klibanov, A. D. Griffiths, and D. A. Weitz, *Proc. Natl. Acad. Sci. U.S.A.* **107**, 4004 (2010).

- <sup>3</sup>K.-H. Kim, R. G. Sanedrin, A. M. Ho, S. W. Lee, N. Moldovan, C. A. Mirkin, and H. D. Espinosa, *Adv. Mater.* **20**, 330 (2008).
- <sup>4</sup>J.-G. Lee, H.-J. Cho, N. Huh, C. Ko, W.-C. Lee, Y.-H. Jang, B. S. Lee, I. S. Kang, and J.-W. Choi, *Biosens. Bioelectron.* **21**, 2240 (2006).
- <sup>5</sup>L. Mugherli, O. N. Burchak, L. A. Balakireva, A. Thomas, F. Châtelain, and M. Y. Balakirev, *Angew. Chem., Int. Ed.* **48**, 7639 (2009).
- <sup>6</sup>P. O. B. Mark Schena, D. Shalon, and R. W. Davis, *Science* **270**, 467 (1995).
- <sup>7</sup>I. Takeuchi, J. Lauterbach, and M. J. Fasolka, *Mater. Today* **8**, 18 (2005).
- <sup>8</sup>W.-K. Choi, E. Lebrasseur, M. I. Al-Haq, H. Tsuchiya, T. Torii, H. Yamazaki, E. Shinohara, and T. Higuchi, *Sens. Actuators, A* **136**, 484 (2007).
- <sup>9</sup>C. Ru, J. Luo, S. Xie, and Y. Sun, *J. Micromech. Microeng.* **24**, 053001 (2014).
- <sup>10</sup>R. D. Piner, *Science* **283**, 661 (1999).
- <sup>11</sup>P. L. Stiles, "Direct deposition of micro- and nanoscale hydrogels using Dip Pen Nanolithography (DPN)," *Nat. Methods* **7**, (2010).
- <sup>12</sup>S. Sekula, J. Fuchs, S. Weg-Remers, P. Nagel, S. Schuppler, J. Fragala, N. Theilacker, M. Franzreb, C. Wingren, P. Ellmark, C. A. K. Borrebaeck, C. A. Mirkin, H. Fuchs, and S. Lenhart, *Small* **4**, 1785 (2008).
- <sup>13</sup>O. A. Nafday and S. Lenhart, *Nanotechnology* **22**, 225301 (2011).
- <sup>14</sup>E. Ueda and P. A. Levkin, *Adv. Mater.* **25**, 1234 (2013).
- <sup>15</sup>M. J. Hancock, F. Yanagawa, Y.-H. Jang, J. He, N. N. Kachouie, H. Kaji, and A. Khademhosseini, *Small* **8**, 393 (2012).
- <sup>16</sup>A. A. Darhuber, S. M. Troian, J. M. Davis, S. M. Miller, and S. Wagner, *J. Appl. Phys.* **88**, 5119 (2000).
- <sup>17</sup>J. Huang, R. Fan, S. Connor, and P. Yang, *Angew. Chem., Int. Ed.* **46**, 2414 (2007).
- <sup>18</sup>R. J. Jackman, D. C. Duffy, E. Ostuni, N. D. Willmore, and G. M. Whitesides, *Anal. Chem.* **70**, 2280 (1998).
- <sup>19</sup>R. Moerman and G. W. K. van Dedem, *Anal. Chem.* **75**, 4132 (2003).
- <sup>20</sup>M. A. Raza, J. Van Swigchem, H. P. Jansen, and H. J. W. Zandvliet, *Surf. Topogr.: Metrol. Prop.* **2**, 035002 (2014).
- <sup>21</sup>P. Olin, S. B. Lindström, T. Pettersson, and L. Wågberg, *Langmuir* **29**, 9079 (2013).
- <sup>22</sup>P. Hao, C. Lv, Z. Yao, and F. He, *Europhys. Lett.* **90**, 66003 (2010).
- <sup>23</sup>S. Dorbolo, D. Terwagne, N. Vandewalle, and T. Gilet, *New J. Phys.* **10**, 113021 (2008).
- <sup>24</sup>S. Courty, G. Lagubeau, and T. Tixier, *Phys. Rev. E* **73**, 045301 (2006).
- <sup>25</sup>J. Seo, S.-K. Lee, J. Lee, J. S. Lee, H. Kwon, S.-W. Cho, J.-H. Ahn, and T. Lee, *Sci. Rep.* **5**, 12326 (2015).
- <sup>26</sup>S. Suzuki, A. Nakajima, K. Tanaka, M. Sakai, A. Hashimoto, N. Yoshida, Y. Kameshima, and K. Okada, *Appl. Surf. Sci.* **254**, 1797 (2008).
- <sup>27</sup>T. Furuta, M. Sakai, T. Isobe, S. Matsushita, and A. Nakajima, *Langmuir* **27**, 7307 (2011).
- <sup>28</sup>S. Varagnolo, D. Ferraro, P. Fantinel, M. Pierno, G. Mistura, G. Amati, L. Biferale, and M. Sbragaglia, *Phys. Rev. Lett.* **111**, 066101 (2013).
- <sup>29</sup>N. Savva and S. Kalliadasis, *J. Fluid Mech.* **725**, 462 (2013).
- <sup>30</sup>J. Hyvälouma, A. Koponen, P. Räsänen, and J. Timonen, *Eur. Phys. J. E* **23**, 289 (2007).
- <sup>31</sup>G. Macdougall and C. Ockerent, *Proc. R. Soc. London* **180**, 151 (1942).
- <sup>32</sup>H. Ren, R. B. Fair, M. G. Pollack, and E. J. Shaughnessy, *Sens. Actuators, B* **87**, 201 (2002).
- <sup>33</sup>See supplementary material at <http://dx.doi.org/10.1063/1.4947008> for details of fabrication process and relationship between capillary number and bond number.
- <sup>34</sup>H. Matsui, Y. Noda, and T. Hasegawa, *Langmuir* **28**, 15450 (2012).